ELSEVIER

Coordination Chemistry Reviews
190–192 (1999) 557–576

COORDINATION CHEMISTRY REVIEWS

www.elsevier.com/locate/ccr

Carbon dioxide interaction with metal atoms: matrix isolation spectroscopic study and DFT calculations

J. Mascetti [a,*], F. Galan [a], I. Pàpai [b]

[a] *Laboratoire de Physico-Chimie Moléculaire, Université Bordeaux I, 351, cours de la Libération, 33405 Talence cedex, France*

[b] *Institute of Isotopes of the Hungarian Academy of Sciences, Spectroscopy Department, PO Box 77, H-1525 Budapest, Hungary*

Accepted 13 March 1999

Contents

* Corresponding author. Tel.: + 33-5-56846360; fax: + 33-5-56848402.
E-mail address: joelle@loriot.lsmc.u-bordeaux.fr (J. Mascetti)

PII: S0010-8545(99)00100-9

Abstract

This paper collects the results obtained in different studies on the interaction of the CO_2 molecule with transition metal atoms, using matrix isolation FTIR spectroscopy and density functional theory (DFT). Late-transition metal atoms (Fe, Co, Ni and Cu) form one-to-one $M(CO_2)$ complexes, while those from the left-hand side in the periodic table (Ti, V, and Cr) insert spontaneously into a CO bond yielding oxocarbonyl species. Owing to isotopic experiments with $^{13}CO_2$ and $C^{18}O_2$, these results allow spectroscopic identification of carbon dioxide bonding modes in organometallic species containing CO_2 moiety. Special attention is paid to the interaction of CO_2 molecule with Ni and Ti atoms. In neat CO_2 matrices, it is shown that CO_2 is side-on coordinated to nickel in a 1:1 complex. The binding energy is weak (18 kcal mol^{-1}). In argon diluted matrices, no reaction occurs, even after annealing. Interestingly, the coordination of CO_2 is promoted by adding N_2 in the rare gas matrix. This is rationalized by comparing the potential energy curves corresponding to the interaction of the Ni atom or the NiN_2 moiety with CO_2. The binding energy is then 32 kcal mol^{-1}. DFT calculations show that Ti inserts with no energy barrier into a CO bond, resulting in an OTiCO insertion product, which is far more stable than any of the possible $Ti(CO_2)$ complexes and reactive towards CO_2. An intrinsic reaction path for the insertion process is investigated.

Keywords: Carbon dioxide; Matrix isolation; FTIR spectroscopy; DFT calculations; Transition metal atoms; Coordination complexes

1. Introduction

The chemical reactivity of atoms with small molecules is a very active area of research. The reactions of transition metal atoms with carbon dioxide are particularly important because this molecule is a potential alternative precursor in organic synthesis, provided that new ways are found to activate it. Activation of carbon dioxide may be accomplished photochemically, electrochemically or catalytically. In most cases, the coordination of CO_2 on a metallic center seems to be the key step for the ultimate reduction of CO_2 [1–5] but the intermediate species formed during the reactions are still unknown. So, this study has been undertaken to learn more about the binding of CO_2 with transition metal atoms and the new species formed.

Results obtained from FTIR (including isotopic studies with $^{13}CO_2$ and $C^{18}O_2$) and density functional theory (DFT) calculations on the $Ni(CO_2)$ and CO_2/N_2 complexes are reported; they were performed at a level of the theory that has recently been applied to a number of transition metal–monoligand system [6]. In the present work, DFT is used to determine the mode of coordination of the CO_2 molecule in the complex, to predict the equilibrium properties of the identified species, to describe the bonding in it, and finally to rationalize the enhanced yield of CO_2 complexation in the presence of N_2 molecules.

The theoretical study of the $Ti + CO_2 \rightarrow OTiCO$ reaction offers the opportunity to compare two different transition metal atoms, one from the left (Ti) and the other from the right (Ni) side of the periodic table. The aims are the understanding of the insertion reaction mechanism and the description of the driving forces in the process.

The paper is organized as follows. In Sections 2 and 3, we describe the experimental and the computational conditions used. Section 4 collects main results previously obtained on the first row transition metals by matrix FTIR spectroscopy and how the use of isotopic labeling can lead to the characterization of the CO_2 coordination modes in organometallic complexes. The $NiCO_2$ study is presented in the fifth section, including vibrational spectra and theoretical results obtained by DFT calculations. The experimental and theoretical results are then discussed in terms of the mode of coordination and bonding in the metallic CO_2 complexes; matrix effects on metal/molecule reactivity are also discussed. The sixth section presents theoretical results obtained for Ti/CO_2 reactivity and proposes a plausible mechanism for the insertion reaction.

2. Experimental

The furnace for metal vaporization and the remainder of the apparatus have been described previously [7,8]. Atoms were generated by directly heating a thin ribbon of metal, strung between two water-cooled electrodes.

Metals were supplied by Goodfellow Metals (minimum purity: 99.98%). CO_2 (99.995%), Ar (99.9995%), and N_2 (99.998%) were supplied by Air Liquide and used without further purification. In addition to $^{12}C^{16}O_2$, isotopically substituted carbon dioxide $^{13}C^{16}O_2$ (99.5% enriched) and $^{12}C^{18}O_2$ (97% enriched), provided by Eurisо-Top, were used to identify reaction products and assign vibrational bands.

The matrix molar ratios used were M/gas = 1/1000. The metal deposition rate was continuously controlled by using a quartz crystal microbalance. Metal and gases were cocondensed at 1 mmol h^{-1} for 2–4 h periods. Matrices were deposited on CsBr windows cooled to 12K by means of a Cryophysics closed cycle refrigerator Cryodine M22. Infrared spectra were recorded with a Bruker 113V interferometer, at a resolution of 2 cm^{-1}.

3. Computational details

The quantum chemical calculations were carried out within the LCGTO-DF formalism [9–13] using the deMon program [14–16]. All properties of the investigated molecules have been obtained at the nonlocal level of theory, using the B-P86 functional [17–19]. All-electron orbital basis sets were employed for all atoms with contraction patterns (63311/5211/41) for Ni and Ti [20] and (5211/411/1) for C and O [21] atoms. The numerical quadrature grid applied has been described previously [22].

The geometries of the molecules were fully optimized without symmetry constraint and Pulay's force method [23] was applied to construct the cartesian force constant matrix, which was then diagonalized to get the normal frequencies and normal vectors. The IR intensities were calculated from numerical derivatives of the dipole moment vector using the double harmonic approximation [24]. The displacement of the cartesian coordinates in the finite-difference procedures was always 0.01 a.u.

The binding energies will be reported with respect to the ground state metal atom and the geometry optimized ground state ligands. The binding energies and the reaction energies were always corrected for the zero point energy (ZPE) contributions estimated from the calculated harmonic frequencies.

Due to the near-degeneracy of the ground state and low-lying excited states for titanium calculations, the virtual orbitals were allowed to mix into the occupied space in the self-consistent field (SCF) procedure by using fractional occupations for orbitals close to the Fermi level. The smear parameter was always 0.3 eV but the total energies for the optimized structures were always recalculated without smearing.

4. FTIR study of CO_2 reactivity towards transition metal atoms

4.1. Matrix isolation results

The different possible bonding modes of CO_2 on transition metals can be summarized as follows: η^2-attachment to one C=O bond: side-on coordination;

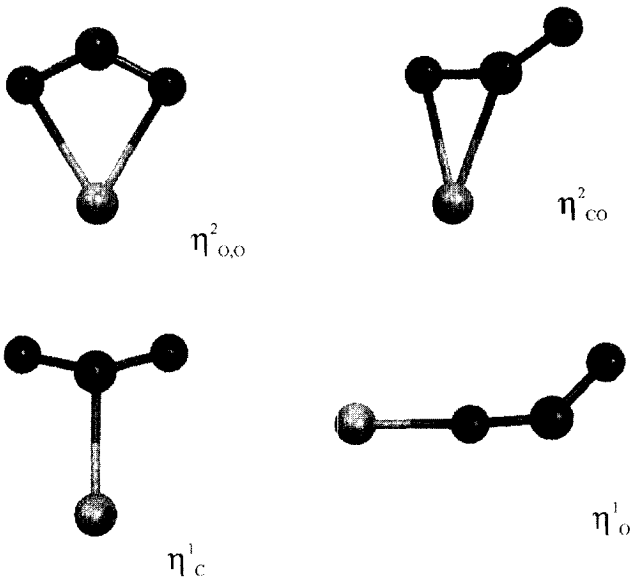

Fig. 1. Main coordination modes of CO_2 on a single transition metal atom.

η^1-attachment to the carbon atom: C-coordination; η^1-attachment to an oxygen atom: end-on coordination (see Fig. 1). The coordination chemistry of CO_2 is often discussed from the standpoint of the solid state structures of stable $L_nM(CO_2)$ complexes [1]. Their significance in catalytic cycles makes them useful models for CO_2 activation, although they are undoubtedly too stable to participate in any catalytic process. To avoid coligands L_n, a convenient route to the preparation of non saturated zerovalent transition metal complexes $M(CO_2)_x$ and their identification by means of vibrational spectroscopy is obtained through the condensation reaction of metal atoms with CO_2 at cryogenic temperatures [25].

Our first experimental results with respect to dilution in argon, thermal activation and isotopic experiments indicated that the late-transition metal atoms (Fe, Co, Ni and Cu) form one-to-one $M(CO_2)$ complexes where CO_2 is bonded in a side-on (Ni), end-on (Cu) or C-coordinated (Fe, Co) manner, while those from the left-hand side in the periodic table (Ti, V, and Cr) insert spontaneously into a CO bond yielding oxocarbonyl species $(O)M(CO)(CO_2)$. Infrared band wavenumbers alone do not allow to discriminate between the different coordination modes (see Fig. 2), but the isotopic shifts are more sensitive to the geometry of the molecule. We were then able to calculate the generalized valence force-field in normal coordinate analysis from a modified version of Schachtschneider's program [26]. All modes were calculated by using internal coordinates. Results showed that the force constants of coordinated CO_2 are significantly decreased (by 50%) compared to free CO_2 and that the OCO angle is highly bent (typically between 120 and 150°).

For example, in the case of $CuCO_2$, further calculations [27] have shown that only the end-on complex (C_s symmetry, *cis* form, $\alpha(OCO) = 133°$) is found to be stable with respect to $Cu - CO_2$ fragments by 6 kcal mol^{-1}. It is characterized by an important charge transfer from copper to CO_2 with the unpaired electron located at the carbon atom.

4.2. Characterization of CO_2 organometallic compounds

This FTIR matrix isolation study led to the conclusion that, if $\Sigma\Delta\nu$ represents the sum of the frequency shifts observed on ν(C=O) (ν_3) and ν(CO) (ν_1) stretching modes in isotopically labeled ^{13}C and ^{18}O CO_2 metal complexes, one expects the following relationships: $\Sigma\,\Delta\nu(^{13}C) > \Sigma\,\Delta\nu(^{18}O)$ with $\Sigma\,\Delta\nu(^{18}O) < 60\ cm^{-1} \Rightarrow$ side-on coordination, $\Sigma\,\Delta\nu(^{13}C) > \Sigma\,\Delta\nu(^{18}O)$ with $60 < \Sigma\,\Delta\nu(^{18}O) < 70\ cm^{-1} \Rightarrow$ C-coordination (in this case, the frequency splitting $\nu_3 - \nu_1$ is small, namely lower than 400 cm^{-1}), $\Sigma\Delta\nu(^{13}C) < \Sigma\Delta\nu(^{18}O)$ with $\Sigma\Delta\nu(^{18}O) > 70\ cm^{-1} \Rightarrow$ end-on coordination (in this case, the out-of-plane bending mode γ(CO), located in the 500–650 cm^{-1} region, exhibits also preponderant ^{18}O frequency shift, in opposition to side-on and C-coordinated compounds, for which ^{13}C shift is larger, namely $\Delta\gamma(^{13}C) = 10$ to 20 cm^{-1} vs. $\Delta\gamma(^{18}O) = 5\ cm^{-1}$).

The availability of FTIR spectroscopy makes then possible to correlate structure with spectroscopic properties, especially with the help of isotopic labeling. The use of ^{13}C and ^{18}O isotopic enrichment allows unequivocal spectroscopic identification

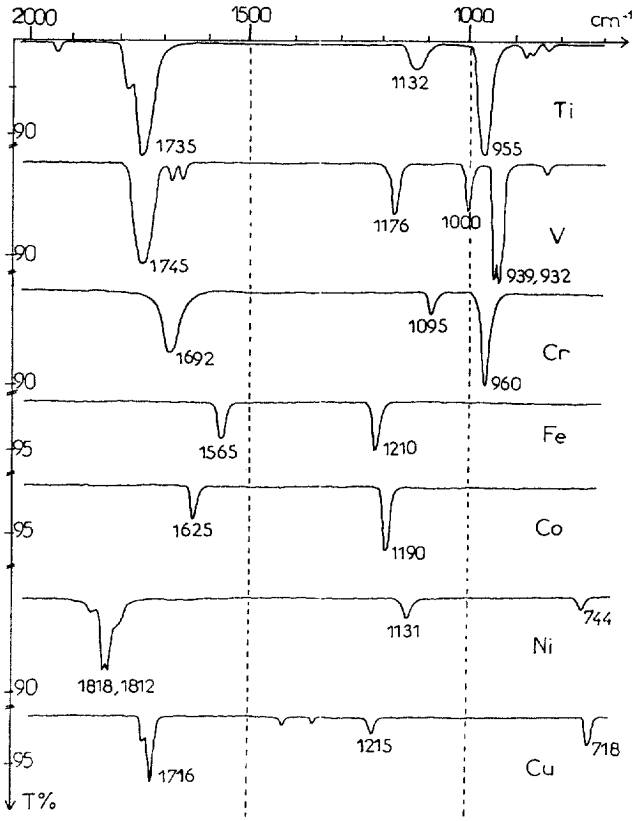

Fig. 2. IR spectra of the condensation reaction products of transition metal atoms in neat CO_2 matrices at 10 K ($M/CO_2 = 1/1000$).

of coordinated CO_2, confirmation of its source, and probe of the bonding in CO_2 complexes. Characterization of CO_2 coordination mode in $Mo(CO_2)_2(PMe_3)_4$ (side-on), $Fe(CO_2)(PMe_3)_4$ (side-on with a shorter metal–carbon bond), and $Cp_2Ti(CO_2)(PMe_3)$ (side-on) has been made, together with evaluation of valence force-field for each compound [28–30]. Significant new insights have also been obtained on dynamic behaviour of $Ni(CO_2)(PCy_3)_2$ [31]. This compound has been shown to exist both with a side-on and an end-on forms, at solid state and in solution; these two isomers are responsible for the fluxionality observed by NMR studies. The availibility of such FTIR studies on labeled compounds has also permitted elucidation of the oxygen transfer process in peroxocarbonates mimicking monooxygenases [32]. We have proved that formation of peroxocarbonate $RhOOC(O)O(Cl)(P)_3$ from CO_2 and $RhCl(\eta^2\text{-}O_2)(P)_3$ proceeds through O–O bond cleavage and CO_2 insertion. O-transfer to ancillary phosphine ligand involves the Rh-linked O atom of the peroxo group of $RhCl(CO_4)(P)_3$.

5. Results and discussion for nickel/carbon dioxide system

Owing to the important role played by nickel in catalytic processes involving carbon dioxide reduction reactions [2,4], we decided to study more accurately the Ni + CO_2 system [33], both by matrix isolation spectroscopy and DFT calculations.

5.1. Experimental results

5.1.1. FTIR results in CO_2 and CO_2/Ar matrices

Only bands from free CO_2 were detected in spectra of diluted argon matrices. Fig. 3 shows the infrared spectrum of nickel atoms condensed in a neat CO_2 matrix: it consists of a set of bands located at 1850(sh), 1818(s), 1812(s) and 1794(sh) cm^{-1}, together with four other weaker absorptions at 1170(w), 1131(m), 750(sh) and 744(w) cm^{-1}. This spectrum remained unchanged up to 106 K, the sublimation point of the CO_2 matrix. At this temperature, two very broad bands appeared at 2050 and 750 cm^{-1}, that can be respectively assigned to carbonyl ν(CO) and metal oxide ν(NiO) stretching modes. From the profiles of these bands, which are sharp for those at 1818, 1812, 1131 and 744 cm^{-1} or broad for those at 1850, 1794, 1170 and 750 cm^{-1}, it is obvious that two different $Ni(CO_2)_n$ complexes (A and B, respectively) exist in the matrix, the second one (B) being less abundant.

The FTIR spectrum of the Ni/$^{13}CO_2$ deposit shows, besides free $^{13}CO_2$ absorptions, bands that are easily correlated with those previously observed in non-labeled matrices: 1815 (which is the average value of the 1818, 1812 cm^{-1} doublet), 1131 and 744 cm^{-1} are respectively shifted by 42, 15 and 14 cm^{-1}, whereas weaker absorptions at 1850, 1794 and 1170 cm^{-1} are respectively shifted by 48, 42 and 16 cm^{-1}.

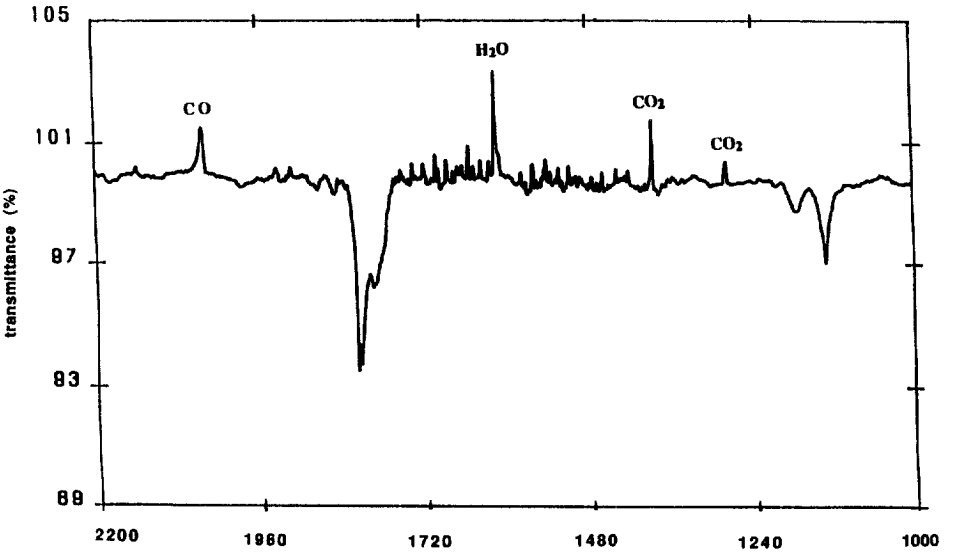

Fig. 3. FTIR spectrum (ν in cm^{-1}) of Ni/CO_2 (1/1000) matrix at 10 K.

Experiments with $C^{18}O_2$ gave similar results with a set of bands at 1803, 1775 and 1747 cm^{-1}, leading to isotopic shifts of 47, 40 and 47 cm^{-1} for the three ν(C=O) modes observed in neat CO_2 matrices. For the ν(CO) modes, the two absorptions at 1170 and 1131 cm^{-1} were shifted by 21 and 18 cm^{-1}, whereas the OCO bending vibration was shifted by 28 cm^{-1} to 716 cm^{-1}.

Similar experiment with a mixture of $C^{16}O_2/C^{18}O_2$ led to a spectrum with a quadruplet at 1812, 1771, 1792, and 1752 cm^{-1}, showing that the $Ni(CO_2)_n$ complexes formed have a 1:1 stoichiometry. In this region, after annealing at 106 K, one doublet appeared at 2050, 2035 cm^{-1} and another doublet was observed at 758 and 738 cm^{-1}, that gave evidence for the reduction of CO_2 to CO, as we previously described [25].

5.1.2. Experimental results in CO_2/N_2 matrices

In order to compare the reactivity of nickel atoms towards carbon dioxide in different media, we decided to study condensation experiments in dinitrogen matrices (concentration ratio: $CO_2/N_2 = 1/10$).

The reactivity of N_2 towards nickel atoms is well known [34,35] and four $Ni(N_2)_n$ complexes have been described with $n = 1$–4.

As expected, the FTIR spectrum of the deposit is dominated by the strong absorptions of $Ni(N_2)_4$ at 2172, 2166 and 281 cm^{-1} but additional bands appear in the ν(NN), ν(C=O), ν(CO), δ(OCO) and low frequency regions. These bands can be divided in two groups, depending on their behaviour during annealing experiments: 2060(m), 1901(sh), 1895(sh), 1884(s), 1851(m), 1792(w, br), 1151(m),1096(m), 725(m), 708(w), 561(w) and 514(w) cm^{-1}, decrease, and 2220(w), 2118(w), 2098(w), 1863(m), 1822(vw), 486(w), 399(w) and 270(w) cm^{-1}, increase during annealing of the matrix. All the bands vanish above 45 K, except for $Ni(N_2)_4$ and two new absorptions at 1996 and 1944 cm^{-1}. Dinitrogen has a phase transition at 35 K, temperature above which it is no longer a good matrix medium [36]: nickel atoms aggregate and broad bands are observed on the spectra.

Unlike with $Ni/CO_2/Ar$ matrices, the presence of bands in the carbonyl stretching region implies the formation of CO_2 complexes in $Ni/CO_2/N_2$ deposits. As already observed for systems such as $Li/C_2H_4/N_2/Ar$ [37], the presence of dinitrogen promotes the coordination of carbon dioxide to nickel atoms. Bands located at 2060, 1884, 1851, 1151, 1096, 725, 708, 561 and 514 cm^{-1} can be associated to two different mixed $nickel/CO_2/N_2$ complexes (C and D).

No nickel aggregates were detected in electronic spectra and no absorption could be assigned to monometallic terminal carbonyl complexes $Ni(CO)_n$ ($n = 1$–4) [38], mixed compounds $Ni(CO)_n(N_2)_{4-n}$ [39] nor nickel surface species [40].

5.2. Theoretical results

5.2.1. The $Ni(CO_2)$ complex

We carried out geometry optimization for the singlet and triplet states for all the possible structures of $Ni(CO_2)$ complex and calculated the harmonic vibrational frequencies and IR intensities at their equilibrium geometries. The obtained results are given in Table 1.

Table 1
Relative stabilities, optimized geometries and IR spectra of various structures of $Ni(CO_2)$ [a]

	η^2_{CO}		η^1_C		η^1_O	
	Single	Triple	Single	Triple [b]	Single	Triple
ΔE	0.0	14.8	17.8	15.1	23.8	20.5
R(NiC)	1.823	1.945	1.759	1.953		
R(NiO)	1.826	2.163		2.195	1.744	2.737
R(CO^1)	1.288	1.248	1.237	1.244	1.186	1.181
R(CO^2)	1.201	1.202	1.237	1.202	1.184	1.175
α(OCO)	144.6	149.3	151.2	149.8	179.0	179.8
α(NiOC)	–	–	–	–	176.5	139.2
ω_1	1901 (539)	1947 (384)	1830 (532)	1953 (379)	2365 (661)	2363 (753)
ω_2	1087 (99.0)	1154 (239)	1169 (260)	1161 (236)	1264 (270)	1314 (1.4)
ω_3	702 (129)	607 (398)	808 (161)	596 (406)	379 (9.5)	618 (21)
ω_4	532 (0.9)	514 (1.7)	507 (3.7)	510 (1.1)	349 (8.4)	609 (15)
ω_5	523 (2.5)	298 (0.5)	322 (25)	282 (0.3)	346 (7.4)	90 (1.2)
ω_6	284 (4.2)	162 (4.1)	i 304	137 (4.1)	219 (0.2)	62 (1.2)

[a] Units: bond lengths (Å), angles (°) and energies (with respect to sing η^2_{CO}) in kcal mol^{-1}. The calculated equilibrium parameters for free CO_2 are: R(CO) = 1.177 Å, ω_1 = 2374(601), ω_2 = 1321(0), ω_3 = 630(25).

[b] Geometry optimization from a η^1_C initial geometry yields η^2_{CO} structure. Optimized parameters of the obtained η^2_{CO} structure are given to illustrate the numerical uncertainty due to the incompleteness of the integration grid.

The singlet η^2_{CO} is found to be the most stable form, all other structures lie at least 15 kcal mol^{-1} higher in energy. Comparing the calculated properties of the coordinated CO_2 ligand with those of the free CO_2 molecule, we see that CO_2 is only slightly distorted in the η^1_O coordination, whereas it undergoes significant structural changes in all of the other cases.

5.2.2. The $Ni(CO_2)(N_2)_n$ (n = 1, 2) complexes

Two different mixed N_2/CO_2 complexes: $Ni(CO_2)(N_2)$ and $Ni(CO_2)(N_2)_2$, were considered in modelling the effect of dinitrogen molecules on the complexation of CO_2. Based on the unambiguous stability of the η^2_{CO} isomer in the case of the binary $Ni(CO_2)$ complex, we assumed a side-on CO_2 coordination in both mixed complexes and fully optimized their geometries. The equilibrium structures and the frequencies of $Ni(CO_2)(N_2)$ and $Ni(CO_2)(N_2)_2$ are given in Table 2 along with those of the singlet η^2_{CO} $Ni(CO_2)$ complex.

Both complexes are nearly planar with roughly linear N_2 coordination. The CO_2 coordination in the mixed complexes is very similar to that in η^2_{CO} $Ni(CO_2)$, however, the CO_2 ligand appears to be a bit less distorted with respect to free CO_2 than in the binary complex (Table 3). Consequently, the CO stretching frequencies are shifted towards higher values by 50–70 cm^{-1} as compared to those in η^2_{CO} $Ni(CO_2)$, but interestingly, the OCO bending frequency is hardly affected by the N_2 coordination. The effect of the second N_2 molecule on the CO_2 coordination seems

Table 2
Calculated properties for $Ni(CO_2)(N_2)$ and $Ni(CO_2)(N_2)_2$ [a]

	$Ni(CO_2)(N_2)$	$Ni(CO_2)(N_2)_2$	$Ni(CO_2)$
R(NiC)	1.890	1.924	1.823
R(NiO)	1.855	1.910	1.826
R(C–O)	1.269	1.263	1.288
R(C=O)	1.194	1.199	1.201
α(OCO)	149.3	148.4	144.6
R(NiN)	1.731	1.774/1.892 [b]	–
R(NN)	1.133	1.129/1.125	–
α(NiNN)	176.1	175.3/165.1	–
α(CNiN)	–	108.7/141.5	–
α(NNiN)	–	108.4	–
ω_1 (asym CO str)	1975 (568)	1965 (571)	1901 (539)
ω_2 (sym CO str)	1132 (177)	1145 (193)	1087 (99)
ω_3 (OCO bend)	701 (176)	689 (257)	702 (129)

[a] Units: bond lengths (Å), angles (°), wavenumbers (cm^{-1}), and intensities (in parentheses).
[b] The first and second numbers refer to the right and left side NiN_2 units, respectively.

to be less important: the CO bond lengths vary by less than 0.01 Å, the OCO valence angle by less than one degree, and there is only about a 10 cm^{-1} shift in the CO_2 frequencies when going from $Ni(CO_2)(N_2)$ to $Ni(CO_2)(N_2)_2$.

5.3. Discussion

5.3.1. The $Ni(CO_2)$ complex

Infrared spectra show the low yield of reaction of nickel towards CO_2 since the maximum absorption of the most intense bands are about 10%. All the observed frequencies are in the ranges expected for coordinated CO_2, although the ν(C=O)

Table 3
Net Mulliken atomic charges and Mayer bond orders for η^2_{CO} $Ni(CO_2)$ and CO_2 molecules

	$Ni(CO_2)$	CO_2
Mulliken charges		
Ni	+0.29	
O^{C-O}	−0.28	−0.18
C	+0.17	+0.36
$O^{C=O}$	−0.18	−0.18
Mayer bond orders		
NiC	0.81	
NiO	0.66	
C–O	1.38	2.18
C=O	2.03	2.18

modes are usually located at lower wavenumbers than 1800 cm^{-1}. The band shapes, annealing experiments and isotopic shifts showed that two different species are formed, both of them with a 1:1 stoichiometry: $Ni(CO_2)$.

The theoretical results suggest that the CO_2 coordination in the $Ni(CO_2)$ complex is side-on, all other isomers being much less stable. Since the predicted vibrational frequencies for the singlet state η^2_{CO} complex are reasonably close to the observed frequencies, we can conclude that the most abundant 1:1 complex (A), observed in neat CO_2 matrices, is the singlet state η^2_{CO} $Ni(CO_2)$. DFT calculations probably overestimate the $\nu_3 - \nu_1$ splitting for both η^2_{CO} and η^1_C isomers, but we must bear in mind that they do not take into account the 'matrix' effect. If argon matrices can be considered as 'good' matrix media (weak potential energy), neat carbon dioxide matrices can induce stronger effects on the isolated species, leading to larger frequency shifts, especially of the asymmetric stretching mode ν(C=O), which is very sensitive to polar effects. Compared to the gas phase or a noble gas matrix, the frequency is then lowered, as is usually observed for carbonyl compounds in polar solvents [41].

The calculated IR intensities are also in line with the observed spectra: the band corresponding to the asymmetric stretching ν(C=O) is the most intense, and the symmetric stretching ν(CO) and bending δ(OCO) bands have similar intensities.

The 26 valence electrons in the ground state ($^1A'$) η^2_{CO} $Ni(CO_2)$ molecule are associated with nine a′ and four a″ doubly occupied molecular orbitals. Among the CO_2 orbitals, 2π is the highest lying occupied CO_2 orbital localized on the two O atoms (lone pairs), whereas $3\pi^*$ is the first virtual CO_2 orbital. It is an antibonding combination of the $p\pi$ carbon and oxygen atomic orbitals.

Most of the $Ni(CO_2)$ orbitals are pure CO_2 or Ni orbitals with only a slight (usually about 5%) admixture with the other moiety, however the 6a′ ($2\pi + 3d$) and 7a′ ($3d + 3\pi^*$) orbitals are mixtures of metal and ligand orbitals. The former is composed of 17% Ni (3d) and 83% CO_2, the latter has 55% Ni (predominantly 3d) and 45% CO_2. The CO_2 contributions to 6a′ and 7a′ have essentially 2π and $3\pi^*$ character respectively, so one can say that 6a′ corresponds to a $CO_2 \rightarrow Ni$, while 7a′ to a $Ni \rightarrow CO_2$ charge transfer, indicating that the Ni–CO_2 bond can be viewed as a dative π bond, just as in $Ni(C_2H_4)$ or NiCO (see Fig. 4). Since the charge donation from the metal to CO_2 is considerably larger than that in the opposite direction, the Ni atom has a net positive charge and the CO_2 ligand has an anionic character. Because of the partial occupation of the $3\pi^*$ CO_2 orbitals in the complex, the CO bonds (and especially the ones interacting directly with the Ni atom) are weakened as seen from the calculated bond orders, or from the shifts in the CO_2 frequencies upon coordination.

The hybridization of the 3d and 4s orbitals (8a′ and 9a′) polarizes the Ni s electrons away from the ligand in order to reduce the Pauli-repulsion between the 4s and the occupied CO_2 orbitals. The hybridization involves the Ni 4p orbitals as well, resulting in a non-negligible 4p Ni population in the complex (the electron configuration of the nickel atom is $3d^{8.98}4s^{0.61}4p^{0.12}$).

The binding energy of the ground state side-on complex is calculated to be $D_0 = 21.1$ kcal mol^{-1}. Assuming the same BSSE as we obtained for the $Ni(C_2H_4)$

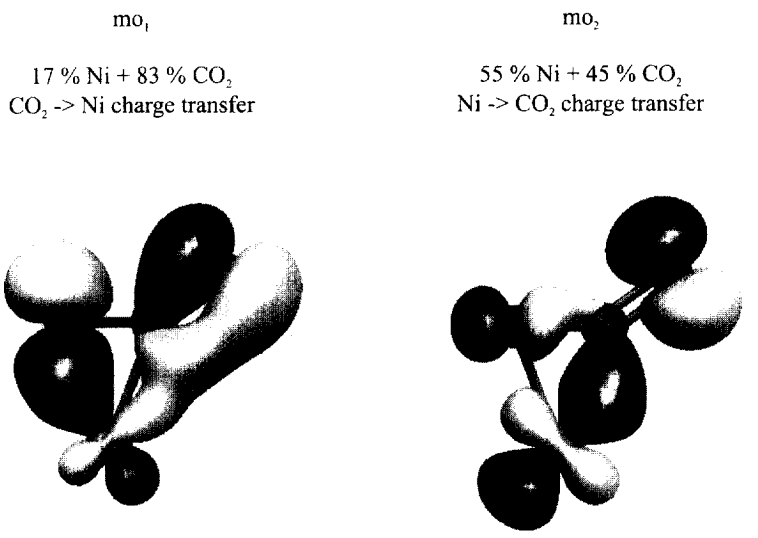

Fig. 4. The bonding orbitals of η^2(C,O) Ni(CO_2).

molecule [42] and correcting D_0 for this error, we get 17.5 kcal mol^{-1} for the binding energy. This is about half the value calculated for Ni(C_2H_4), showing that despite the similarities in the bonding in the two complexes, Ni(CO_2) is thermodynamically far less stable than Ni(C_2H_4), which might be one of the reasons that CO_2 gives a considerably lower yield upon complexation with Ni than C_2H_4 does.

5.3.2. Role of dinitrogen on CO_2 coordination

The XY stretching modes splitting and the YXY bending frequency are known to be related to the value of the YXY angle in any non linear triatomic molecule XY_2 [43]. In the mixed CO_2/N_2 species, the OCO angle can then vary from 148 to 153°. Taking into consideration the very high reactivity of N_2 towards nickel compared to that of CO_2, the most probable stoichiometry is then Ni(CO_2)(N_2)$_n$ with $n = 1$ or 2 if CO_2 is side-on coordinated, or possibly Ni(CO_2)(N_2)$_3$ if CO_2 is end-on bonded to the nickel atom. The mixed Ni/CO_2/N_2 complexes observed in the matrix exhibit no further reactivity by annealing up to 35 K and the only other compound formed is Ni(N_2)$_4$, which is a tetrahedral, stable and unreactive saturated complex [34,35]. The most probable reaction mechanism is then the following: $Ni + nN_2 + CO_2 \rightarrow Ni(N_2)_n + CO_2 \rightarrow Ni(N_2)_n(CO_2)$ with $n < 4$. After condensation at 10 K, these species are stable enough to keep CO_2 coordinated in a dinitrogen environment.

The theoretical results obtained for the Ni(CO_2)(N_2) and Ni(CO_2)(N_2)$_2$ complexes support this conclusion in that the CO stretching frequencies are (blue or red)-shifted and the OCO bending frequency is (red or blue)-shifted in the mixed complexes relative to those in the binary complex, as observed experimentally. However, we are unable to specify the number of coordinated N_2 molecules in the mixed species. On the other hand, we can look at the energetics of the coordination

of CO_2 to the different $Ni(N_2)_n$ species, which are presumably formed prior to CO_2 coordination because of the excess N_2. We get 32.2 and 3.5 kcal mol^{-1} for the energies of the $Ni(CO_2)(N_2) \rightarrow Ni(N_2) + CO_2$ and $Ni(CO_2)(N_2)_2 \rightarrow Ni(N_2)_2 + CO_2$ reactions, respectively, indicating that the CO_2 coordination to $Ni(N_2)$ is theormodynamically favoured over its coordination to a ground state Ni atom, whereas the coordination to $Ni(N_2)_2$ is very unlikely. The low CO_2 binding energy obtained for $Ni(CO_2)(N_2)_2$ is due to the fact that the equilibrium structure of the $Ni(N_2)_2$ molecule is linear and the bending of this unit upon the CO_2 coordination requires a considerable amount of energy.

In order to understand the increased CO_2 binding energy in $Ni(CO_2)(N_2)$ versus $Ni(CO_2)$, we calculated the potential energy curves corresponding to the interaction of the s^1d^9 (^3D) Ni atom, and the singlet $Ni(N_2)$ molecule with a gas phase (linear) CO_2 molecule, as shown in Fig. 5. The difference in the shape of the two curves is quite striking. The Ni–CO_2 interaction appears to be repulsive, while the interaction energy for $Ni(N_2)$–CO_2 continuously decreases when approaching CO_2, reaching a minimum at around $y = 2.0$ Å, where ΔE is about 7 kcal mol^{-1}. The $Ni(N_2)$ orbitals reveal that the coordination of N_2 to Ni atom induces a hybridization of the Ni 4s and 3d orbitals and, as a result, the electron configuration of the Ni atom in $Ni(N_2)$ becomes very similar to that in $Ni(CO_2)$ ($4s^{0.79}3d^{9.02}4p^{0.02}$ in $Ni(N_2)$ and as we saw earlier, $4s^{0.61}3d^{8.98}4p^{0.12}$ in $Ni(CO_2)$). Consequently, the s electrons on the

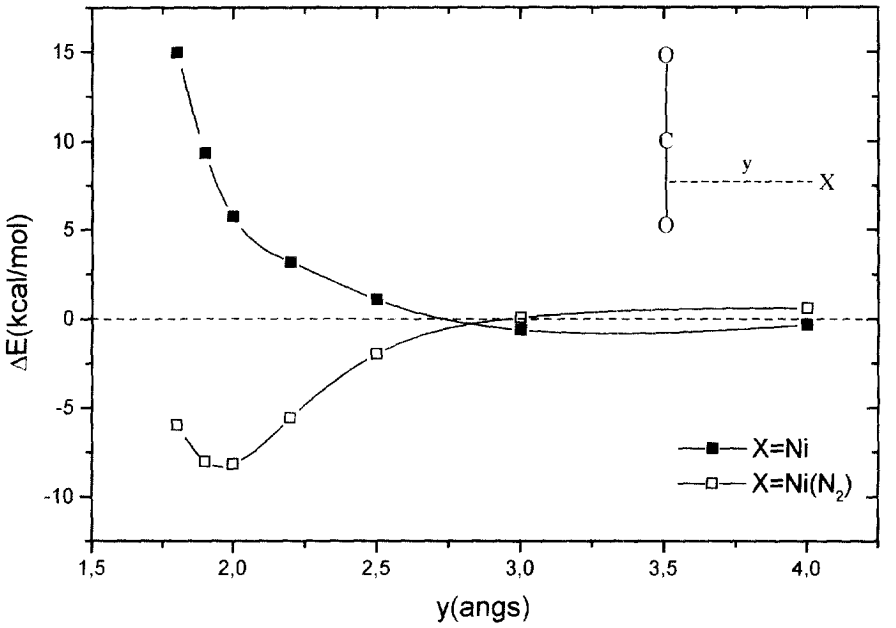

Fig. 5. Interaction of the s^1d^9 (^3D) Ni atom and the singlet state $Ni(N_2)$ molecule with a linear CO_2 molecule. The geometry of the CO_2 molecule and the $Ni(N_2)$ complex are fixed at their equilibrium structures and the distance between the midpoint of the CO bond and the Ni atom is varied. For $CO_2 + Ni(N_2)$, the molecular axes of CO_2 and $Ni(N_2)$ are perpendicular.

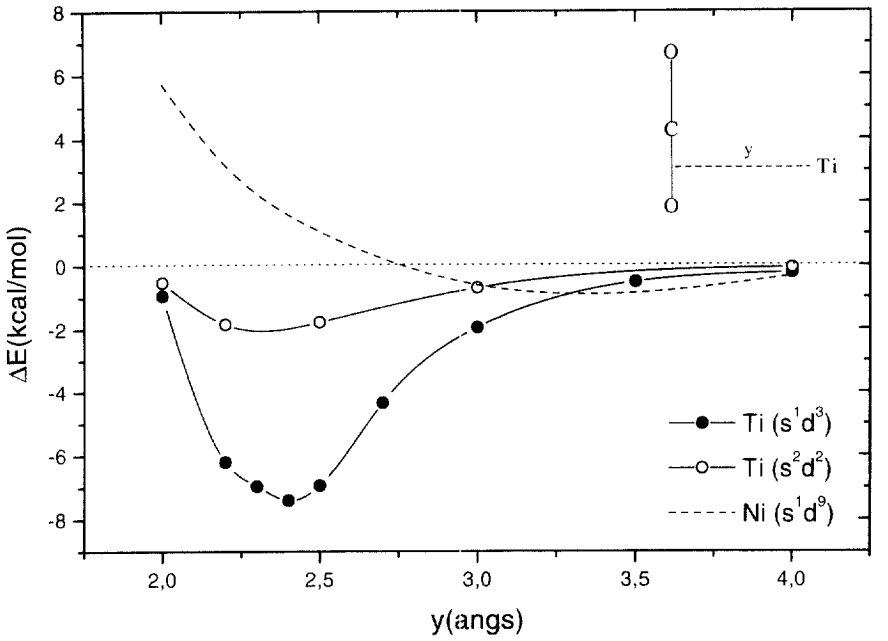

Fig. 6. Interaction of s^2d^2 (^3F) and s^1d^3 (^5F) Ti and s^1d^9 (^3D) Ni atoms with a linear CO_2 molecule. The geometry of the CO_2 molecule is fixed at its equilibrium structure ($R = 1.177$ Å) and the distance between the midpoint of the CO bond and the metal atom is varied.

Ni atom are already polarized away from the approaching CO_2, allowing the metal d_p orbitals to interact with the CO_2 $3\pi^*$ orbitals. Since the metal → ligand charge transfer is not great in $Ni(N_2)$ (0.16 e), the Ni atom in $Ni(CO_2)(N_2)$ can still donate a similar amount of charge to the CO_2 as in $Ni(CO_2)$ (0.25 e vs. 0.30 e). Since the 4s–3d hybridization energy has already been paid in coordinating with N_2, the CO_2 binding energy is higher in $Ni(CO_2)(N_2)$ than in $Ni(CO_2)$.

6. Results and discussion for the titanium/carbon dioxide system

Although several $M + CO_2$ systems have been investigated with various theoretical approaches [27,44–48], none of them addressed the question of metal insertion. This theoretical study focuses on the $Ti + CO_2 \rightarrow OTiCO$ reaction observed in our matrix experiments [25,49] and by another group using laser-ablated Ti atoms [50a].

6.1. The $Ti(CO_2)$ complex

The first step of our study consists in deriving two potential energy curves corresponding to the interaction of s^2d^2 (^3F) and s^1d^3 (^5F) Ti atoms with a linear CO_2 molecule as shown on Fig. 6. These curves cannot describe accurately the

long-range interactions but provide a qualitative picture about the strength of the $M-CO_2$ interaction. We can see a clear difference between the two metals, Ni and Ti; the $Ni-CO_2$ curve is essentially repulsive, while both $Ti-CO_2$ curves have well-defined minima with about 2 and 7 kcal mol^{-1} interaction energies for the triplet and quintet states, respectively. The binding is mostly due to the mixture of Ti 3d and CO_2 $3\pi^*$ orbitals. This orbital is singly occupied and corresponds to a $Ti \rightarrow CO_2$ charge transfer. Therefore, the $Ti-CO_2$ bond has a slight ionic character, which becomes more important when the 'complex' is allowed to relax, as we will see later on. The other component of the $Ti-CO_2$ interaction is the repulsive interaction between the Ti 4s and the occupied CO_2 σ orbitals. The reason the $Ti-CO_2$ interaction is favorable for the quintet state is that the $\sigma-$repulsion is stronger for the s^2d^2 configuration than for the s^1d^3. As for the difference in the nature of the $Ni-CO_2$ and $Ti-CO_2$ curves, we can point out two trends in the atomic properties of transition metal series both indicating that the $3d-3\pi^*$ bonding becomes less dominant for the late transition metals. The first is the strong contraction of the 3d orbitals with respect to the 4s as the atomic number increases, and the second is the increase of the ionization potential of metal atoms along the row (Ti: 6.0 and Ni: 8.7 eV). Four stationary points have been found on the quintet potential energy surface of $Ti(CO_2)$ corresponding to the four possible coordination modes: η^2(O,O), η^2(C,O) (side-on), η^1-C and η^1-O (end-on) and two for the triplet state: η^2(O,O) and η^1-O (end-on). The optimization with initial side-on or C-coordinated structures always led to the spontaneous insertion of Ti into the CO bond, yielding the OTiCO product (see Section 6.2). Interestingly, no $Ti(CO_2)$ complex has been observed in matrix experiments [25,49,50a]. Among these six isomers, the triplet state (O,O) coordination mode is the most stable one; it is separated by at least 14 kcal mol^{-1} from all the others. The binding energy relative to the ground state species ($Ti(s^2d^2) + CO_2(\Sigma_g^+)$) at infinite separation is calculated to be $D_o =$ 34.9 kcal mol^{-1}, lowered by about 4–5 kcal mol^{-1} if BSSE correction is applied. The quintet states of $Ti(CO_2)$ are far less stable (the most stable is bound by only 13 kcal mol^{-1}) and considering that the experimental $s^2d^2 \rightarrow s^1d^3$ excitation energy of Ti is 16 kcal mol^{-1} [51], the quintet states are in fact unbound relative to the ground state species.

6.2. The $Ti + CO_2 \rightarrow OTiCO$ insertion

Geometry optimization for the interaction of the ground state Ti atom and CO_2 with initial η^2(C,O) and η^1-C structures resulted in the insertion of Ti into a C–O bond. It is remarkable that the insertion took place even with an undistorted CO_2 initial geometry, showing that the reaction for breaking the C–O bond has no energy barrier at all. In order to describe the mechanism of the insertion, we will follow the path that connects an arbitrarily chosen initial structure, namely, the one corresponding to the energy minimum of the Ti (s^2d^2) + CO_2 (linear) system to the global minimum of the triplet potential energy surface, which is equivalent to the triplet state of the OTiCO molecule. The minimization algorithm we used in the optimization is the steepest descent gradient method [52]. The variation of the total

energy along the reaction path is depicted on Fig. 7 with some characteristic structures. We can see that the weakly bound Ti–CO_2 system (structure I) is very quickly stabilized as soon as the CO_2 molecule is allowed to relax. The stabilization energy of structure II is already about 30 kcal mol^{-1} with respect to structure I. The immediate bending of the ligand indicates that a significant amount of negative charge is being transferred from the metal to CO_2. Ti atom bears a positive charge equivalent to about 0.5 e^- charge transfer, which hardly changes for the rest of the reaction path. The region between the structures I and II can therefore be viewed as the formation of a quite strong Ti–C bond. The Ti–C bond in structure II is shorter by more than 0.2 Å than Ti–O. This latter bond is strengthened in the next stage of the reaction, and the two bond distances become almost equal in structure III, which therefore corresponds to the triplet state side-on Ti(CO_2) complex. The ΔE energy curve becomes rather flat going from structures III to IV. This is the region where the C–O bond breaks up as seen from the shape of the C–O curve in Fig. 8. The reason the system still stabilizes upon the cleavage of the C–O bond is that the Ti–O bond strengthens considerably; it shortens by 0.2 Å from III to IV and it has double bond character in IV. The other C–O bond is at this point typical for a coordinated carbonyl group. It seems therefore that the energy gain obtained on the formation of the Ti=O and Ti–CO bonds in this step of the reaction exceeds the energy required to cleave the CO bond of CO_2. In the next stage, the energy decreases again to a greater extent. The stabilization of 10 kcal mol^{-1} between

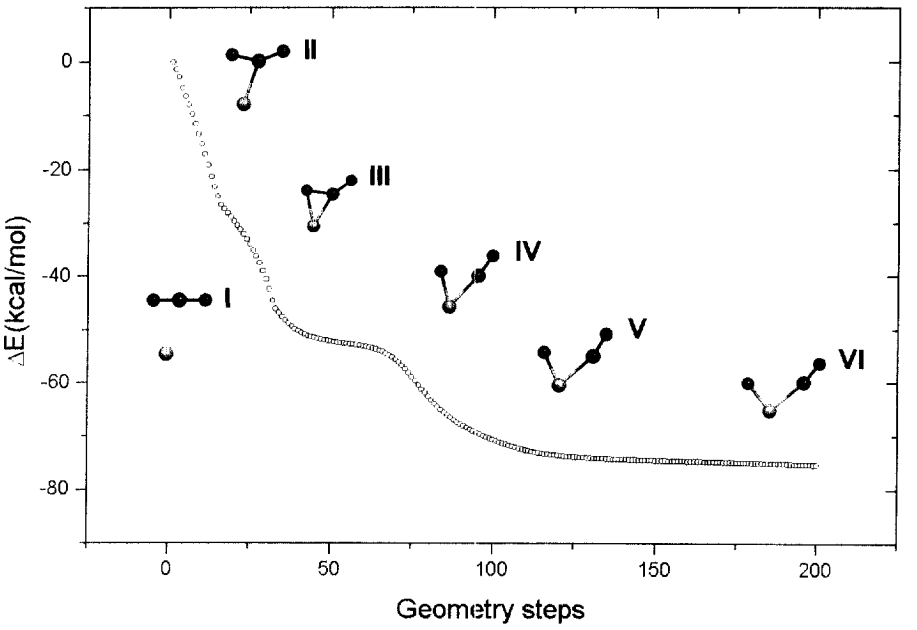

Fig. 7. The variation of the total energy along the Ti(s^2d^2) + $CO_2(^1\Sigma_g^+)$ → OTiCO($^3A'$) reaction path. The energies are given for each even number of geometry steps relative to the initial structure. Structures corresponding to steps numbered 0, 20, 40, 75, 100, and 200 are referred as structures I–VI, respectively.

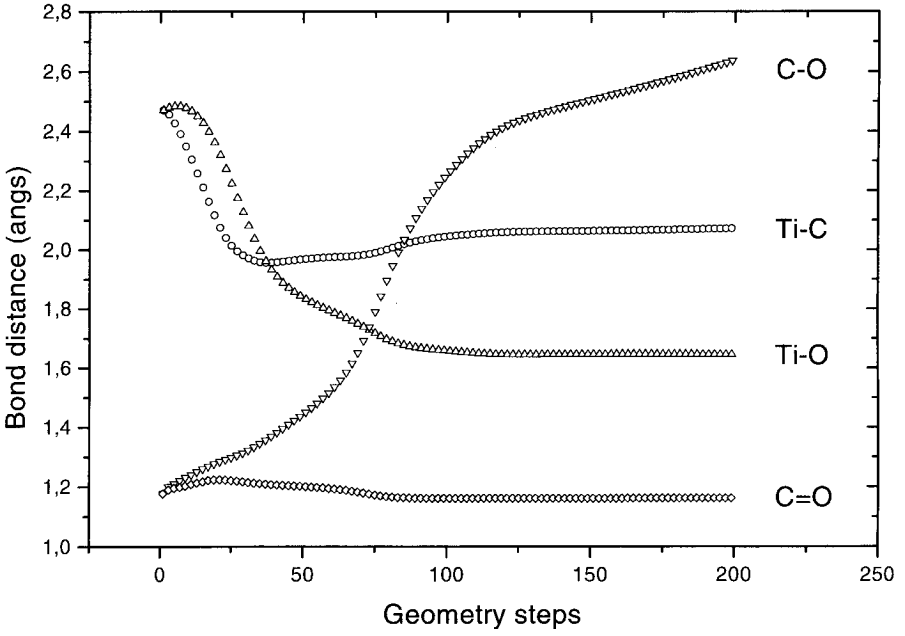

Fig. 8. Bond lengths (Å) as a function of geometry steps for the $Ti(s^2d^2) + CO_2(^1\Sigma_g^+) \rightarrow OTiCO(^3A'')$ reaction.

structures IV and V is related to the opening of the OTiC angle. The TiO bond in V is quite close to that in free TiO; it can therefore be viewed as a TiO-carbonyl complex.

The above analysis suggests a reasonable reaction mechanism for the Ti insertion. In the first step of the reaction, a weakly bound collision complex of ground state Ti and CO_2 is formed followed by a quick relaxation of CO_2 occurring on the time scale of the OCO vibrational period. After the formation of this complex, the system 'rolls' further downhill toward the global minimum, while the CO bond is broken and the strong Ti=O bond is formed. Finally, the OTiCO complex relaxes to its equilibrium structure. The OTi–CO binding energy is calculated to be 23 kcal mol^{-1}. Taking into account that the BP86 functional tends to overestimate the M–CO binding energies by at least 10 kcal mol^{-1} [53], the CO molecule is probably only weakly bound in OTiCO, which may explain the formation of TiO and CO fragments besides the main products in matrix isolation experiments [25,49,50a,b].

The DFT results agree with the experimental ones obtained by matrix isolation FTIR studies: both laser ablated [50a] and thermally evaporated [25] (i.e. with less kinetic energy) Ti atoms insert spontaneously (i.e. with no energy barrier) into the CO bond of the CO_2 molecule. Our matrix studies [25] have also shown that, in neat CO_2 matrices, side-on coordination occurred on the OTiCO insertion product, leading to the formation of the $OTi(CO)(CO_2)$ species. Indeed, our preliminary

DFT calculations show that the interaction of CO_2 with OTiCO leads to the formation of a fairly stable OTi(CO)(CO_2) complex ($D_e(CO_2) = 28$ kcal mol^{-1}), in which CO_2 is side-on coordinated to Ti and the OTiCO and Ti(CO_2) units lie in perpendicular planes. Further calculations on various oxo-Ti(CO_2) complexes are in progress.

7. Conclusions

Matrix isolation FTIR study of the reactivity of transition metal atoms with CO_2 has revealed the important role played by the analysis of isotopic labeling and normal coordinate treatment. For the first time, the metal–CO_2 vibrational modes have been assigned and related force-constants evaluated in organometallic compounds. Owing to their interest in catalytic reactions, special attention has been paid to Ni and Ti reactivity towards CO_2.

FTIR and UV-vis studies have shown that two $NiCO_2$ complexes are formed in neat CO_2 matrices at 10 K. The more abundant one has been fully characterized by density functional calculations with non-local corrections. The binding energy (18 kcal mol^{-1}) shows that this complex is far less stable than 'similar' molecules, like Ni(C_2H_4) or NiCO. The CO_2 coordination mode is found to be side-on, and the OCO angle, 146°, is larger than the values usually encountered in stable side-on CO_2 complexes. Indeed, the reaction yield for the reaction between Ni and CO_2 is very low and no reaction occurs in argon diluted matrices. Interestingly, the coordination of CO_2 is promoted by using N_2 in place of rare gas matrices. This has been rationalized by comparing the potential energy curves corresponding to the interaction of the Ni atom or the Ni(N_2) moiety with CO_2. Coordination of N_2 to Ni atom induces a hybridization of the Ni 4s and 3d orbitals, resulting in more Ni → CO_2 charge transfer in Ni(CO_2)(N_2) than in Ni(CO_2). This study emphases the important roles played by the matrix and the cooperative effects of co-ligands in binding molecules to metal atoms, as already observed in other systems [54].

Both matrix isolation FTIR and DFT studies have shown that the insertion of a ground state Ti atom into a CO bond of carbon dioxide takes place with no activation barrier and the OTiCO molecule is thermodynamically far more stable than any of the possible Ti(CO_2) complexes. We have proposed a plausible reaction mechanism for the insertion and described the structure of the insertion product.

Finally, this study illustrates the advantages of associating theory and experiment in the field of mechanistic investigations of carbon dioxide activation and reactivity. Theoretical investigations are expected to be effective in obtaining information on geometry, electronic structure, bonding nature, and binding energies of transition metal complexes, but important limitations related to correlation effects and spin mutiplicity exist. DFT methods have been proved to be reliable to treat these problems with rather short computational times [6]. Various MO theoretical studies have been previously performed on carbon dioxide complexes of transition metal fragments (see for example Mealli et al. [55] and Sakaki [56]). They have confirmed the validity of the Chatt–Dewar–Duncanson model when applied to carbon

dioxide side-on bonding mode and have proposed a way of predicting the coordination mode of CO_2 in different fragments. In the present work, DFT has been used to determine the mode of coordination of the CO_2 molecule, to predict the equilibrium properties of the identified species, to describe the bonding and the vibrational spectra, and to rationalize the experimental results obtained in matrix media: the enhanced yield of CO_2 complexation on Ni in the presence of N_2 molecules, and the insertion reaction of Ti in CO_2.

Acknowledgements

J.M. and I.P. acknowledge financial support from CNRS and the Hungarian Academy of Sciences.

References

[1] A. Behr, Carbon Dioxide Activation by Metal Complexes, VCH, Weinheim, 1988.
[2] M. Aresta, E. Quaranta, I. Tommasi, New J. Chem. 18 (1994) 133.
[3] P. Braunstein, D. Matt, D. Nobel, Chem. Rev. 88 (1988) 747.
[4] W. Leitner, Coord. Chem. Rev. 153 (1996) 257.
[5] D.H. Gibson, Chem. Rev. 96 (1996) 2063.
[6] R. Fournier, I. Pàpai, in: D. Chong (Ed.), Recent Advances in Computational Chemistry, Part I, World Scientific, Singapore, 1995.
[7] (a) C. Cossé-Mertens, Thèse, Université Bordeaux I, 1981. (b) F. Galan, Thèse, Université Bordeaux I, 1994.
[8] M. Tranquille, Spectra 2000 98 (1984) 43.
[9] H. Sambe, R.H. Felton, J. Chem. Phys. 62 (1975) 1122.
[10] B.I. Dunlap, J.W.D. Conolly, J.R. Sabin, J. Chem. Phys. 71 (1979) 3396.
[11] J. Andzelm, E. Radzio, D.R. Salahub, J. Chem. Phys. 83 (1985) 4573.
[12] R. Fournier, J. Andzelm, D.R. Salahub, J. Chem. Phys. 90 (1989) 6371.
[13] D.R. Salahub, R. Fournier, P. Mlynarski, I. Pápai, A. St-Amant, J. Ushio, in: J. Labanowski, J. Andzelm (Eds.), Density Functional Methods in Chemistry, Springer-Verlag, New York, 1991, p. 77.
[14] A. St-Amant, D.R. Salahub, Chem. Phys. Lett. 169 (1990) 387.
[15] A. St-Amant, Ph.D. Thesis, Université de Montréal, 1991.
[16] C. Daul, A. Goursot, D.R. Salahub, in: C. Cerjan (Ed.), Numerical Grid Methods and Their Application to Schrödinger's Equation, NATO ASI Series, vol. 412, Kluwer, Dordrecht, 1993, p. 153.
[17] A.D. Becke, Phys. Rev. A. 38 (1988) 3098.
[18] J.C. Slater, Quantum Theory of Molecules and Solids, vol. 4, The Self-Consistent Field for Molecules and Solids, McGraw-Hill, New York, 1994.
[19] J.P. Perdew, Phys. Rev. B 33 (1986) 8822; erratum in Phys. Rev. B 38 (1986) 7406.
[20] N. Godbout, J. Andzelm, D.R. Salahub, E. Wimmer, Can. J. Chem. 70 (1992) 560.
[21] F. Sim, D.R. Salahub, S. Chin, M. Dupuis, J. Chem. Phys. 95 (1991) 4317.
[22] I. Pápai, J. Chem. Phys. 103 (1995) 1860.
[23] P. Pulay, in: H.F. Schaefer III (Ed.), Applications of Electronic Structure Theory, Modern Theoretical Chemistry, vol. 4, Plenum Press, New York, 1977.
[24] A. Komornicki, J.W. McIver, J. Chem. Phys. 70 (1979) 2014.
[25] J. Mascetti, M. Tranquille, J. Phys. Chem. 92 (1988) 2177.

[26] J.H. Schachtschneider, R.G. Snyder, Spectrochim. Acta 19 (1963) 117.
[27] R. Caballol, E.S. Marcos, J. Barthelat, J. Phys. Chem. 91 (1987) 1328.
[28] C. Jegat, J. Mascetti, New J. Chem. 15 (1991) 17.
[29] C. Jegat, M. Fouassier, J. Mascetti, Inorg. Chem. 30 (1991) 1521.
[30] C. Jegat, M. Fouassier, M. Tranquille, J. Mascetti, Inorg. Chem. 30 (1991) 1529.
[31] C. Jegat, M. Fouassier, M. Tranquille, J. Mascetti, I. Tommasi, M. Aresta, F. Igold, A. Dedieu, Inorg. Chem. 32 (1993) 1279.
[32] M. Aresta, I. Tommasi, E. Quaranta, C. Fragale, J. Mascetti, M. Tranquille, F. Galan, M. Fouassier, Inorg. Chem. 35 (1996) 4254.
[33] F. Galan, M. Fouassier, M. Tranquille, J. Mascetti, I. Papai, J. Phys. Chem. A 101 (1997) 2626.
[34] H. Huber, E.P. Kundig, M. Moskovits, G.A. Ozin, J. Am. Chem. Soc. 95 (1973) 332.
[35] W. Klotzbucher, G.A. Ozin, J. Am. Chem. Soc. 97 (1975) 2672.
[36] A. Becker, W. Langel, S. Maass, E. Knoezinger, J. Phys. Chem. 97 (1993) 5525.
[37] L. Manceron, M. Hawkins, L. Andrews, J. Phys. Chem. 90 (1986) 4987.
[38] R.L. De Kock, Inorg. Chem. 10 (1971) 1205.
[39] E.P. Kundig, M. Moskovits, G.A. Ozin, Can. J. Chem. 51 (1973) 2737.
[40] R.P. Eischens, Spectrochim. Acta 21 (1965) 1295.
[41] K. Nakamoto, Infrared Spectra of Inorganic and Coordination Compounds, 4th edition, Wiley Interscience, New York, 1986.
[42] The BSSE for $Ni(C_2H_4)$ was estimated to be 3.6 kcal mol^{-1}. It is quite reasonable to assume a similar error for the side-on $Ni(CO_2)$ complex since the distances are similar in $Ni(CO_2)$ and in $Ni(C_2H_4)$ and both calculations were carried out using the same functional and the same basis sets.
[43] G. Herzberg, Infrared and Raman Spectra of Polyatomic Molecules, 7th edition, van Nostrand, New York, 1956.
[44] G.H. Jeung, Mol. Phys. 65 (1988) 669.
[45] G.H. Jeung, Mol. Phys. 67 (1989) 747.
[46] G.H. Jeung, Chem. Phys. Lett. 232 (1995) 319.
[47] S. Sirois, M. Castro, D.R. Salahub, Int. J. Quant. Chem. S28 (1994) 645.
[48] M. Sodupe, V. Branchadell, A. Oliva, J. Phys. Chem. 99 (1995) 8567.
[49] J. Mascetti, R. Fournier, I. Papai, J. Phys. Chem. A 101 (1997) 4465.
[50] (a) G.V. Chertihin, L. Andrews, J. Am. Chem. Soc. 117 (1995) 1595, (b) G.V. Chertihin, L. Andrews, J. Am. Chem. Soc. 119 (1997) 7350.
[51] R.L. Martin, P.J. Hay, J. Chem. Phys. 75 (1981) 4539.
[52] H.B. Schlegel, in: K.P. Lauley (Ed.), Ab-Initio Methods in Quantum Chemistry-I, Wiley, New York, 1987.
[53] C. Adamo, F. Lelj, J. Chem. Phys. 103 (1995) 10605.
[54] K.K. Sunil, Chem. Phys. Lett. 195 (1992) 355.
[55] C. Mealli, R. Hoffmann, A. Stockis, Inorg. Chem. 23 (1984) 56.
[56] S. Sakaki, in: I. Bernal (Ed.), Stereochemical Control, Bonding and Steric Rearrangements, Elsevier, Amsterdam, 1990, p. 95.